Conjunctival Myxoid Lesions: Clinical-Pathologic Multiparametric Analysis, Including Molecular Genetics (An American Ophthalmological Society Thesis)

TATYANA MILMAN, DIVA R. SALOMAO, CRISTIANE M. IDA, DANIEL R. CAPIZ CORREA, HANS E. GROSSNIKLAUS, QIANG ZHANG, ROSE A. HAMERSHOCK, CAROL SHIELDS, JERRY A. SHIELDS, IRVING RABER, CHRISTOPHER J. RAPUANO, RAVI PATEL, AND RALPH C. EAGLE JR

• PURPOSE: To evaluate the clinical and pathologic characteristics of conjunctival myxoid lesions, with specific focus on PRKAR1A studies, in order to distinguish neoplastic conjunctival myxoma from other myxoid conjunctival lesions.

• METHODS: A retrospective, interventional, multicenter study of all patients with conjunctival myxoma, conjunctival stromal tumor, or reactive fibromyxoid proliferation diagnosed during 1988–2018. Patient and family medical histories and clinical and pathologic characteristics of excised lesions were assessed.

• RESULTS: There were 28 patients with conjunctival myxoid lesions diagnosed as myxoma (16/28), conjunctival stromal tumor (10/28), or reactive fibromyxoid proliferation (2/28). The patients with abundant myxoid matrix lesions (14/28, 50%) were younger (mean 49 [range 23–68] years) than those with scant-to-moderate myxoid matrix lesions (14/28, mean 61 [range 18–82] years; $P = .04$). Abundant myxoid matrix lesions more likely contained predominantly stellate cells (6/14 [43%] vs 0/14 [0%]; $P = .05$) and fibrillar collagen (13/14 [93%] vs 2/14 [14%]; $P < .0001$), conforming to the standard morphologic definition of myxoma. Absence of PRKAR1A protein expression was found in 2 lesions with morphologic features of myxoma (2/14, 14%), 1 of which demonstrated a pathogenic mutation in the *PRKAR1A* gene. There was no difference between the lesions with respect to other clinical and pathologic parameters.

• CONCLUSIONS: *PRKAR1A* plays a role in the development of a subset of conjunctival myxomas, particularly in tumors fulfilling stringent morphologic criteria for myxoma. With the exception of PRKAR1A studies, current immunohistochemical panels cannot reliably distinguish between neoplastic conjunctival myxomas and other myxoid lesions, underscoring the importance of morphology in establishing accurate diagnosis. NOTE: Publication of this article is sponsored by the American Ophthalmological Society. (Am J Ophthalmol 2019;205:115–131. © 2019 Elsevier Inc. All rights reserved.)

MYXOID TUMORS OF THE CONJUNCTIVA ARE UNcommon lesions with controversial nosology and overlapping morphology. Reflecting these challenges, various terms have been applied to conjunctival myxoid lesions, including "conjunctival myxoma," "conjunctival stromal tumor (COST)," and, more recently, "conjunctival myxoid stromal tumor," on the basis of their morphologic, ultrastructural, and immunohistochemical patterns.[1–11]

Although previously not evaluated by molecular genetic methods, a small subset of conjunctival myxoid tumors are believed to be true neoplasms associated with Carney complex (CNC), a hereditary cancer syndrome characterized by spotty mucocutaneous pigmentation, myxomas of various tissues (including the heart), other benign and malignant tumors, and endocrine hyperactivity.[4,5,12] The ophthalmic manifestations of CNC can appear before embolic events originating from cardiac myxomas, underscoring the importance of timely diagnosis.[4,5] More than 70% of the patients with CNC diagnoses carry mutations on the *PRKAR1A* gene, encoding the regulatory subunit type I alpha of cAMP-dependent protein kinase A.[12] *PRKAR1A* mutations have been identified in two-thirds of CNC-associated cardiac myxomas and in one-third of isolated cardiac myxomas.[13] Similarly,

AJO.com Supplemental Material available at AJO.com.

Accepted for publication Apr 18, 2019.

From the Department of Ophthalmology, Thomas Jefferson University, Philadelphia, PA, USA (T.M., Q.Z., R.A.H., C.S., J.A.S., I.R., C.J.R., R.P., R.C.E.); Department of Pathology, Wills Eye Hospital, Philadelphia, PA, USA (T.M., R.C.E.); Department of Laboratory Medicine and Pathology, Mayo Clinic, Mayo Clinic College of Medicine and Science, Rochester, MN, USA (D.R.S., C.M.I.); Orbit and Oculoplastics Department, Hospital de la Luz, Mexico City, Mexico (D.R.C.C.); Department of Ophthalmology, Ocular Oncology and Pathology Section, Emory Eye Center, Emory University School of Medicine, Atlanta, GA (H.E.G.); Biostatistics Consulting Core, Vickie and Jack Farber Vision Research Center, Wills Eye Hospital, Philadelphia, PA (Q.Z., R.A.H.); Ocular Oncology Service, Wills Eye Hospital, Philadelphia, PA, USA (C.S., J.A.S.); and Cornea Service, Wills Eye Hospital, Philadelphia, PA, USA (I.R., C.J.R., R.P.).

Inquires to Tatyana Milman, Department of Pathology, Wills Eye Hospital, 840 Walnut St, Philadelphia, PA 19107, USA; e-mail: tmilman@willseye.org

0002-9394/$36.00
https://doi.org/10.1016/j.ajo.2019.04.027

PRKAR1A mutations have been identified in odontogenic and cutaneous myxomas.[14,15] Additionally, loss of PRKAR1A expression in immunohistochemical stains has been documented in approximately one half of cardiac and odontogenic myxomas and has been found to be useful in screening cardiac myxomas for CNC.[13,14]

The challenges in classification and diagnosis of myxoid lesions are not unique to the conjunctiva. In analogous superficial sites, the skin and oral mucosa, numerous investigations have focused on the histopathologic criteria that enable distinction of neoplastic myxoma from reactive and degenerative mucinosis.[16–21] The parameters assessed include the lesion's size and shape, vascular and mast cell density, and collagen fiber pattern.[16–21]

We hypothesize that similar to those of cutaneous and oral mucosal sites, conjunctival myxoid lesions fall into 2 main categories: 1) benign neoplastic myxomas that can be either isolated (nonsyndromic) or associated with CNC (syndromic) and 2) reactive fibromyxoid proliferations and myxoid degenerations. We hypothesize further that neoplastic myxomas can be separated from reactive myxoid conjunctival lesions on the basis of their morphology and immunohistochemistry and that *PRKAR1A* mutation studies can discriminate between the syndromic and nonsyndromic conjunctival myxomas. Herein, we analyze conjunctival myxoid lesions with morphologic, immunohistochemical, and molecular genetic criteria used in the evaluation of cardiac and odontogenic myxomas, cutaneous myxoma, and mucinosis and correlate these data with clinical characteristics to enable distinction between conjunctival syndromic and nonsyndromic myxomas and other myxoid lesions.

METHODS

• **CASE SELECTION AND REVIEW:** After Wills Eye Hospital institutional review board approval, a retrospective review of Wills Eye Hospital, Emory Eye Center, and Mayo Clinic Pathology Department records was conducted to identify all biopsies with tissue available for histopathologic evaluation that originated from patients with conjunctival myxoma, conjunctival stromal tumor, and conjunctival fibromyxoid proliferation diagnoses given during January 1, 1988–January 1, 2018. The lesions with tissue unavailable for pathologic evaluation were excluded from the study. The original pathologic diagnoses were rendered independently by 4 pathologists (T.M., R.C.E., H.E.G., and D.R.S.) and these diagnoses were recorded without alteration.

The pathologic diagnosis of reactive fibromyxoid proliferation was rendered to lesions occurring at sites of prior surgery for an unrelated disease process. The original pathologic diagnosis of myxoma and COST was dependent on the date of diagnosis and morphologic and immunohistochemical features of the lesion. Before the emergence of COST as an entity in 2012,[9] all primary myxoid proliferations were diagnosed as myxoma. According to the characterization of histopathologic and immunohistochemical features of COST by Herwig and associates,[9] the diagnosis of COST was rendered to conjunctival tumors composed predominantly of spindle cells with occasional pseudonuclear inclusions and multinucleated giant cells in a background of ropey collagen and a scant myxoid matrix. Alternatively, the diagnosis of COST was rendered to myxoid tumors expressing CD34, vimentin, and CD68, irrespective of cellular, collagen, and myxoid matrix patterns.

Clinical data collected included patient age at the time of surgery, sex, clinical features of the tumor, duration of symptoms, ocular history, ocular and systemic medications, interventions, personal and family history of cancer and immune mediated diseases, and outcomes. Specifically, the medical records were reviewed for features of CNC (Supplemental Table).

• **HISTOPATHOLOGY AND IMMUNOHISTOCHEMISTRY:** Routine sections stained with hematoxylin-eosin, Alcian blue, and Hale colloidal iron were prepared from paraffin-embedded, formalin-fixed tissues. When sufficient tissue for immunohistochemical evaluation was available, the immunostaining was performed by using standard immunohistochemical techniques with the following primary antibodies: monoclonal mouse anti-human CD68 (prediluted; DAKO, Santa Clara, California, USA), monoclonal mouse anti-human CD34 (prediluted; Leica Biosystems Inc, Buffalo Grove, Illinois, USA), monoclonal mouse anti-human vimentin (diluted 1:60; DAKO), monoclonal mouse anti-human factor XIIIa (diluted 1:300; Thermo Fisher Scientific, Waltham, Massachusetts, USA), polyclonal rabbit anti-human S100 (prediluted; DAKO), monoclonal mouse anti-human SOX10 (prediluted; Biocare, Pacheco, California, USA), monoclonal mouse anti-human RB1 (diluted 1:50; Thermo Fisher Scientific), monoclonal mouse anti-human SMA (undiluted 1:600; DAKO), and monoclonal mouse anti-human PRKAR1A (diluted 1:2000; OriGene, Rockville, Maryland, USA). Peroxidase activity was visualized by applying diaminobenzidine solution containing 0.05% H_2O_2. Sections were counterstained with a modified Mayer hematoxylin, dehydrated, cleared, and mounted. Appropriate positive and negative controls were run with each batch.

Morphologic parameters assessed included the lesion's circumscription, cell morphology, mast cell and vascular density, non-mast cell inflammatory infiltrate quantification and characterization, amount of myxoid stroma, and morphology of intervening collagen. The cell morphology was expressed in the order of predominating cell type (stellate, spindle, and round). The presence of intranuclear

TABLE 1. Clinical Features of Patients with Conjunctival Myxoid Lesions

Pt No.	Age (y)/ Sex	Systemic Disease	Ocular Disease	Family History Cancer	Symptom Duration (mo)	Eye	Location Quadrant	Location Region	Size (mm)	Shape, Consistency	Color	Clinical Impression	Surgery	Recurrence/ Follow-up (mo)
1[a]	23/M	CNC	Eyelid myxoma	CNC	4	OD	Superior	Tarsus and orbit	20	DS, cystic	Yellow	Cyst	Excision	Yes/12
2	62/M	NA	No	No	1	OS	Inferonasal	Bulbar and orbit	NA	DS, gelatinous	Yellow-pink	Lipomatous	Exc+C	NA
3	58/F	No	No	No	120	OS	Nasal	Limbus	9	DS, cystic	Pink	Lymphoid	Excision	NA
4	45/M	No	FB trauma	No	24	OD	Nasal	Limbus	6	DS, cystic	NA	Myxoma	Exc+C	No/6
5	50/M	No	No	No	24	OS	Nasal	Limbus	5	DS, cystic	NA	Cyst	I+D	NA
6	56/M	No	OSD	No	90	OD	Temporal	Limbus	8	DS, cystic	NA	Cyst	Excision	No/1
7	34/M	No	NA	No	NA	OD	Temporal	Limbus	8	DS, cystic	NA	Cyst	Excision	NA
8	63/M	No	FB trauma	No	90	OD	Temporal	Limbus	10	DS, gelatinous	NA	Cyst	Excision	No/1
9	64/M	No	NA	NA	18	OD	IT	Limbus	NA	NA	NA	Tumor	Excision	NA
10	50/M	NA	NA	NA	NA	OS	Inferior	Limbus	NA	NA	NA	Tumor	Excision	NA
11[b]	31/M	No	No	No	24	OS	Nasal	Limbus	12	DS, cystic	Yellow	Cyst	Excision	No/132
12	63/F	Breast carcinoma	OSD	Lung carcinoma	18	OS	Nasal	Limbus	10	DS, gelatinous	NA	Myxoma	Exc+C	No/12
13	51/M	No	FB trauma	No	12	OD	IT	Limbus	13	DS, gelatinous	Yellow-white	Myxoma	Exc+C	No/144
14	50/M	No	Strabismus surgery	No	2	OS	Temporal	Limbus	8	DS and papillomatous, gelatinous	NA	SCC	Exc+C	NA
15	48/M	Sarcoidosis	No	NA	NA	OS	NA	Bulbar	5	DS, cystic	NA	Cyst	Excision	NA
16	57/M	NA	NA	NA	NA	OD	NA	Bulbar	NA	NA	NA	NA	Excision	NA
17	80/F	No	No	No	2	OS	NA	Plica and caruncle	NA	DS, cystic	NA	Cyst	Excision	No/4
18	75/M	Bladder, lung carcinoma	FB trauma	No	6	OD	NA	Plica and caruncle	8	Pedunculated, fibrovascular	Pink-red	PG	Exc+C	No/10
19	82/F	Thyroid nodules	FB trauma, OSD	No	2	OS	NA	Plica and caruncle	6	DS, cystic	Yellow-pink	Lipomatous	Exc+C	No/12
20[c]	48/M	NA	NA	NA	NA	OS	Nasal	Bulbar	12	Fibrovascular	Red	Lymphoid	Excision	NA
21	68/M	No	NA	No	NA	OD	NA	NA	3	DS, cystic	NA	Cyst	Excision	No/21
22	38/F	No	NA	No	NA	OD	NA	NA	3	DS, cystic	NA	Cyst	Excision	No/13
23	78/F	NA	NA	No	NA	OD	NA	NA	6	NA	NA	Tumor	Excision	No/25
24	18/M	NA	NA	No	8	OD	Nasal	Bulbar	3	Fibrovascular	Red	Scleritis	Excision	Yes/2

Continued on next page

TABLE 1. Clinical Features of Patients with Conjunctival Myxoid Lesions (*Continued*)

Pt No.	Age (y)/ Sex	Systemic Disease	Ocular Disease	Family History Cancer	Symptom Duration (mo)	Eye	Location Quadrant	Location Region	Size (mm)	Shape, Consistency	Color	Clinical Impression	Surgery	Recurrence/ Follow-up (mo)
25	60/M	No	NA	No	18	OD	NA	Plica and caruncle	9	DS, cystic	NA	Cyst	Excision	No/5
26	62/M	NA	NA	No	NA	OD	Temporal	Bulbar	7	NA	NA	Tumor	Excision	No/8
27	63/M	No	Pterygium excision	No	112	OS	Temporal	Limbus	6	DS, fibrovascular	Pink-red	cSCC	Exc+C	No/20
28	61/M	NA	cSCC excision	NA	4	OS	Temporal	Limbus	NA	NA	NA	FH	Excision	NA

CNC = carney complex; cSCC = conjunctival squamous cell carcinoma; DS = dome-shaped; Exc+C = excision with cryotherapy; FH = fibrous histiocytoma; I+D = incision and drainage; IT = inferotemporal; FB = foreign body; NA = not available; OD = ocular dexter; OS = ocular sinister; OSD = ocular surface disease; PG = pyogenic granuloma.

[a]Patient no. 1 was previously reported by Kennedy and associates.[4]

[b]Patient no. 11 was previously reported by Demirci and associates.[3]

[c]Patient no. 20 was previously reported by Auw-Haedrich and associates.[10]

cytoplasmic pseudoinclusions (vacuoles), multinucleation, and floret-type giant cells was recorded. The collagen pattern was expressed in the order of predominance as fibrillary, ropey, and dense (compact). The amount of myxoid matrix was recorded as abundant (collagen and cells suspended in pools of mucin), moderate (approximately equal proportions of mucin and collagen with cellular constituents), and sparse (barely perceptible mucin). The mast cell and vascular densities were expressed as number of mast cells and vessels in 10 high power fields (HPFs). The constituent cells of the inflammatory infiltrate in each lesion were recorded, and the inflammatory infiltrate was quantified by assessing hot spots within the lesion as follows: 0 (no inflammatory cells), 1+ (rare cells, 1–20 cells/HPF), 2+ (mild, 21–50 cells/HPF), and 3+ (moderate, 51–100 cells/HPF).

Immunohistochemical stains were interpreted semiquantitatively for staining intensity (0 none, 1+ mild, 2+ moderate, and 3+ strong) and percentage of immunoreactive cells (0 none, 1+ for 1%–25% immunoreactive, 2+ for 26%–50% immunoreactive, 3+ for 51%–75% immunoreactive, and 4+ for 76%–100% immunoreactive).

• ***PRKAR1A* GENE SEQUENCING:** One hematoxylin and eosin–stained section and 10 unstained, 5-mm–thick tissue sections were prepared on glass slides from the paraffin-embedded, formalin-fixed blocks from the 4 myxomas that had sufficient tissue available for analysis, including 2 myxomas that demonstrated absence of PRKAR1A protein expression and 2 myxomas with retained PRKAR1A expression. Tumor tissue was macrodissected for tumor enrichment (range 20%–90%). DNA was extracted from the entire tissue on the slide using a QIAamp DNA FFPE Tissue Kit (QIAGEN, Germantown, Maryland, USA) with few modifications.[22] A next-generation sequencing (NGS) library was prepared by using a QIAseq Targeted DNA custom amplicon-based panel designed to interrogate 150 central nervous system tumor-associated genes, including all 10 coding exons and intron-exon boundaries of the *PRKAR1A* gene (NM212472.1). Paired-end 2 x 151–bp sequencing was performed on an Illumina HiSeq 2500 instrument (Illumina Inc, San Diego, California, USA). NGS data were processed through custom bioinformatics pipelines developed to detect single nucleotide variants and small insertions-deletions (<50 bp) with at least a 15% variant allelic frequency. DNA sequence alterations were visualized by using Alamut Visual, version 2.7 rev. 2 (Interactive Biosoftware, Rouen, France), and alterations showing a minimum of 100x depth of coverage were reviewed and classified as benign polymorphisms, variants of unknown significance, or pathogenic mutations on the basis of publicly available genetic databases and literature.

• **STATISTICAL ANALYSIS:** Summary statistics were reported for demographics, clinical data, histopathology,

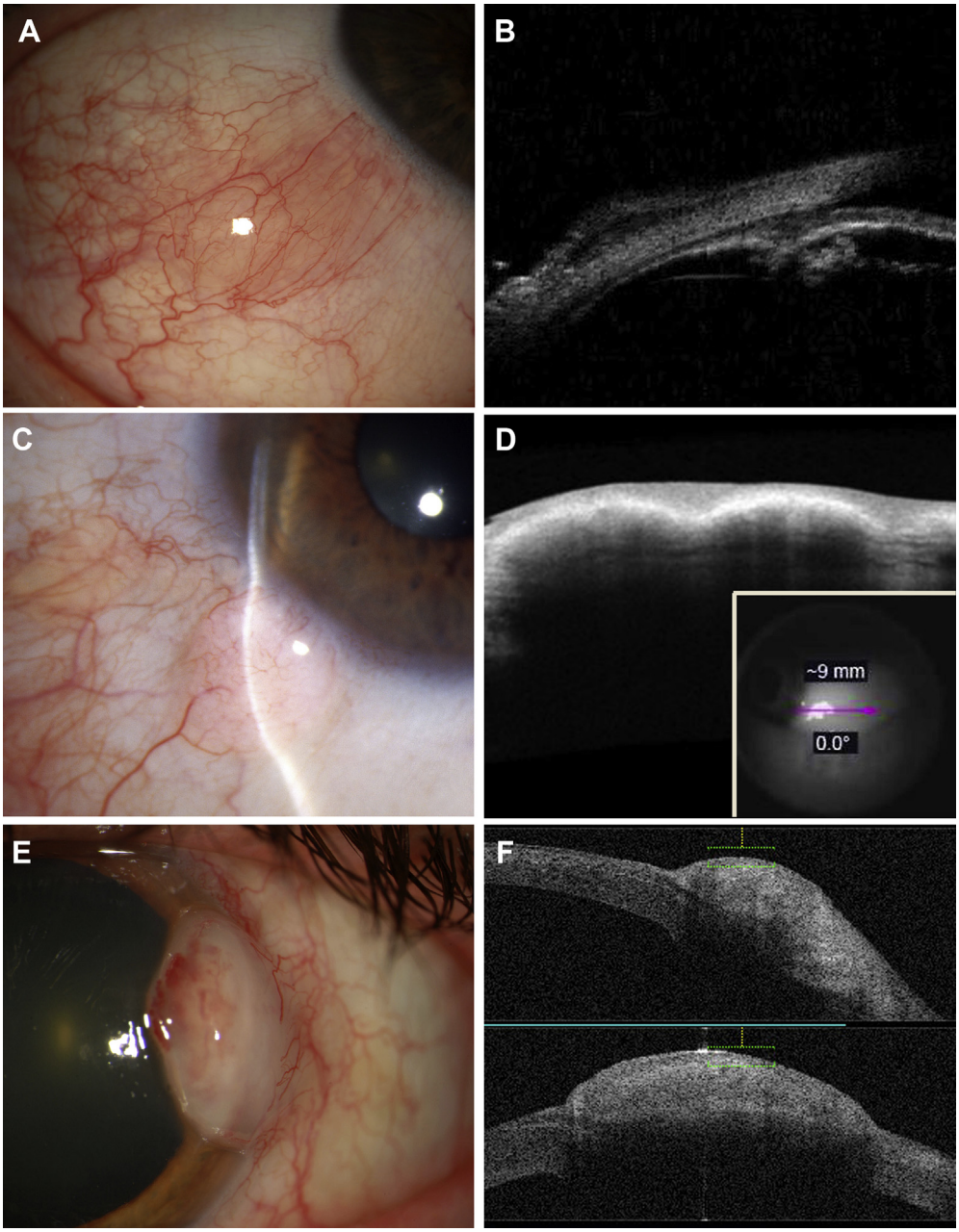

FIGURE 1. The spectrum of clinical features of conjunctival myxoid lesions. A: Lesion with classic histopathologic features of myxoma appears clinically as a yellow-pink, dome-shaped, cystic-appearing, gelatinous, translucent, inferotemporal limbal nodule with fine vascularity. B: The corresponding anterior segment ultrasound biomicroscopy documents an epibulbar mass with a hypoechoic center. C: Lesion with histopathologic features of conjunctival stromal tumor appears as a white-pink, dome-shaped, solid, somewhat gelatinous, right inferotemporal limbal nodule. D: Anterior segment optical coherence tomography of a lesion with similar histology demonstrates a left inferotemporal limbal conjunctival stromal mass with a hyperreflectile anterior border and lucent center. E: Lesion with histopathologic diagnosis of reactive fibromyxoid proliferation after surgery for pterygium appears as a dense, dome-shaped, fibrovascular corneoscleral limbal nodule. F: The corresponding anterior segment optical coherence tomography demonstrates a hyperreflectile homogeneous epibulbar mass.

immunohistochemistry, and molecular genetic information on a patient level. Fisher exact and rank sum tests were used to determine differences between groups for categorical variables. *t* tests (2 groups) and analysis of variance (3 groups) were used for normally distributed continuous variables. Kruskal-Wallis test was used for nonnormally distributed continuous variables. All statistical analyses were performed in SAS V9.4 (SAS Institute Inc, Cary,

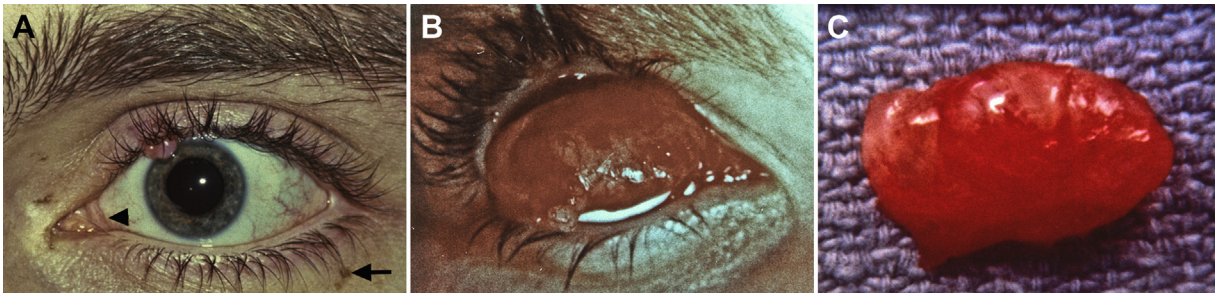

FIGURE 2. Clinical and gross features of Carney complex–associated conjunctival myxoma (Patient 1). A: Ocular stigmata of a patient with Carney complex. Left upper eyelid margin has (biopsy-proven) myxoma and spotty pigmentation of the skin (arrow) and plica semilunaris (arrowhead). B: Pink, vascular mass involving right tarsal conjunctiva. C: The resected mass is well-circumscribed, translucent, and vascular.

North Carolina, USA), and 2-sided *P* values <.05 were considered statistically significant.

RESULTS

• **CLINICAL CHARACTERISTICS:** Review of pathology medical records identified 28 patients with conjunctival myxoid lesions bearing the diagnosis of myxoma (16/28, 57%), conjunctival stromal tumor (10/28, 36%), and reactive fibromyxoid proliferation (2/28, 7%). The clinical characteristics of the patients are summarized in Table 1 (complete histories are not available for all patients). The clinical appearance of the lesions is documented in the Figure 1.

There were 21 male and 7 female patients; their mean age was 55 (median 58, range 18–82) years. The right eye was involved in 15 patients (54%) and the left in 13 patients (46%). The lesions appeared as translucent cystic and gelatinous (18/22, 82%) or fibrovascular (4/22, 18%) nodules, light yellow (5/10, 50%) or pink-to-red (5/10, 50%) in color in a dome-shaped configuration (18/22, 82%) ranging 3–20 (median 8) mm in size. The lesions were most frequently localized to the limbal (14/25, 56%) or bulbar (6/25, 24%) conjunctiva, where they predominantly involved the interpalpebral temporal or inferotemporal (9/22, 41%) and nasal or inferonasal (8/22, 36%) quadrants. The tarsal conjunctiva and adjacent eyelid margin were involved in 1 tumor (1/25, 4%), and 4 tumors were situated in the plica semilunaris or caruncle (4/25, 16%). Extension into the adjacent orbit was observed in 2 tumors (2/25, 8%).

The duration of symptoms ranged 1–120 (median 18) months. Six patients (6/14, 43%) had no history of prior ocular disease. History of nonsurgical trauma (foreign bodies) in the affected eye was documented in 5 of 17 patients (29%). Three patients (3/17, 18%) had history of prior surgery at the site of the lesion. Ocular surface disease (dry eye syndrome, blepharitis, conjunctivochalasis) was documented in 3 of 16 patients (19%).

Five patients (5/20, 25%) had a personal history of other tumors. One patient fulfilled the diagnostic criteria for CNC (atrial myxoma, bilateral testicular calcifying Sertoli cell tumor, cutaneous nodules [including histopathologically confirmed eyelid myxoma], cutaneous lentigines, and family history of CNC-associated tumors) (Supplemental Table, Figure 2).[4]

The most common clinical diagnosis was cyst (11/27, 41%). Myxoma was suspected clinically in 3 of 27 patients (11%). Nineteen lesions (19/28, 68%) were removed by simple excision, 8 were managed by excision with cryotherapy (8/28, 28%), and 1 was unroofed and excised at the slit lamp (1/28, 4%). Patient follow-up ranged 1–144 (median 8) months. Two lesions (2/17, 12%) recurred within 12 months of diagnosis. None of the lesions behaved in a malignant fashion.

• **HISTOPATHOLOGY:** The histopathologic features of the lesions are summarized in Table 2 and documented in Figures 3-7. Assessment of tumor circumscription was hindered in most cases by the tissue orientation and completeness of surgical excision. In excisions with a peripheral rim of uninvolved tissue, the lesional cells and stroma blended into the surrounding tissue without a sharply circumscribed margin. The lesions were composed of varying proportions of spindle, stellate, and round or ovoid cells with occasional intranuclear cytoplasmic pseudoinclusions, and multinucleated cells, such as floret-type giant cells, in a background of fibrillary, ropey, or dense collagen fibers and abundant to scant myxoid stroma. Vascular density ranged 8–160 (mean 68) vascular channels/10 HPFs. Mast cells, ranging 0–44 (mean 19) cells/10 HPFs were scattered throughout the lesions. The non–mast cell inflammatory infiltrate was generally sparse and consisted of macrophages, lymphocytes, and occasional plasma cells, predominantly in a perivascular distribution. None of the lesions demonstrated significant nuclear pleomorphism, mitotic figures, apoptosis, or necrosis. The resection margins involved tumor tissue in both cases with subsequent recurrence.

TABLE 2. Histopathologic, Immunohistochemical, and Molecular Characteristics of Conjunctival Myxoid Lesions

Pt no.	Initial Diagnosis	Cell Morphology[a]	MNC/FC/VC	Myxoid Matrix	Collagen Pattern[b]	Vessel/ 10 HPF (no.)	Mast Cells/ 10 HPF (no.)	L/M/PC (0–3+)[c]	Immunohistochemical Stains (Intensity/% Immunoreactive)[d]									Molecular Studies,
									CD68	CD34	Vimentin	Factor XIIIa	S100	SOX10	RB1	SMA	PRKAR1A	PRKAR1A Mutation
1	Myxoma	St>Sp>R	P/A/P	Abundant	F>Rop	20	18	1+/1+/1+	NA	3+/4+	NA	0	0	0	NA	0	0	Positive
2	Myxoma	St>R>Sp	P/P/P	Abundant	F>Rop	73	31	1+/1+/0	2+/1+	3+/4+	NA	0	0	0	3+/4+	0	3+/3+	NA
3	Myxoma	Sp>St>R	P/P/P	Abundant	F>Rop	160	26	1+/1+/1+	3+/1+	3+/4+	NA	2+/1+	0	0	2+/2+	0	0	Negative
4	Myxoma	St>Sp>R	P/P/P	Abundant	F>Rop	9	12	1+/1+/0	3+/1+	3+/4+	NA	2+/1+	0	0	2+/4+	0	3+/4+	Negative
5	Myxoma	St>Sp>R	P/A/P	Abundant	F>Rop	8	4	1+/1+/0	3+/2+	3+/4+	NA	0	0	0	3+/4+	0	3+/4+	NA
6	Myxoma	Sp>R>St	P/A/P	Abundant	Rop>F	144	44	1+/1+/0	3+/1+	3+/4+	NA	2+/1+	0	0	3+/4+	0	3+/4+	NA
7	Myxoma	Sp>R>St	P/A/P	Moderate	Rop>F	45	3	1+/1+/0	2+/1+	3+/4+	NA	0	0	0	3+/4+	0	3+/4+	NA
8	Myxoma	Sp>R>St	A/A/P	Moderate	Rop >F	110	20	1+/1+/1+	2+/1+	3+/4+	2+/4+	2+/1+	0	0	2+/3+	0	3+/4+	NA
9	Myxoma	Sp>R>St	P/A/P	Moderate	Rop>F	72	40	1+/1+/0	2+/1+	3+/4+	NA	2+/1+	0	0	1+1+	0	3+/3+	NA
10	Myxoma	Sp>R>St	P/P/P	Scant	Rop >F	28	14	1+/1+/1+	2+/1+	3+/4+	NA	0	0	0	1+/2+	0	2+/2+	NA
11	Myxoma	Sp>R>St	P/P/P	Abundant	F>Rop	35	3	1+/1+/0	0	3+/4+	NA	NA	0	0	2+/3+	0	3+/4+	Negative
12	Myxoma	R>Sp>St	P/A/P	Moderate	Rop>F	89	21	1+/1+/1+	NA	3+/4+	NA	0	1+/3+	0	3+/4+	0	3+/4+	NA
13	Myxoma	R>Sp	P/A/A	Abundant	F>Rop	52	21	1+/1+/0	NA	NA	NA	NA	NA	NA	NA	NA	NA	NA
14	Myxoma	Sp>R>St	P/A/P	Abundant	F>Rop	60	20	1+/1+/1+	3+/1+	3+/4+	2+/4+	NA	0	NA	NA	0	NA	NA
15	Myxoma	St>R>Sp	P/A/P	Abundant	F>Rop	NA	NA	NA	NA	3+/4+	NA	NA	0	NA	NA	NA	3+/4+	NA
16	Myxoma	St>Sp>R	P/A/P	Abundant	F>Rop	60	12	1+/1+/0	NA	3+/4+	NA	NA	0	NA	3+/4+	NA	3+/3+	NA
17	COST	Sp>R>St	P/A/P	Scant	Rop>F	42	42	1+/1+/1+	2+/1+	3+/4+	1+/3+	2+/1+	0	0	2+/2+	0	NA	NA
18	COST	Sp>St>R	P/A/P	Scant	Rop>F	48	19	1+/1+/1+	3+/1+	3+/4+	NA	NA	0	0	3+/4+	0	3+/4+	NA
19	COST	Sp>R>St	P/A/P	Scant	Rop>F	68	28	2+/1+/1+	0	3+/4+	NA	NA	0	NA	3+/4+	0	3+/4+	NA
20	COST	Sp>R>St	P/P/P	Abundant	F	110	36	1+/1+/0	3+/2+	3+/4+	3+/4+	3+/3+	0	0	2+/3+	0	3+/3+	NA
21	COST	Sp>R	P/A/P	Abundant	F>Rop	31	12	1+/1+/1+	NA	3+/4+	NA	3+/2+	0	0	2+/3+	0	3+/2+	NA
22	COST	Sp>R>St	P/A/P	Abundant	F	80	14	1+/1+/0	3+/1+	3+/4+	NA	3+/2+	0	0	2+/2+	0	3+/3+	NA
23	COST	Sp>R	P/A/P	Moderate	F>Rop	126	18	2+/1+/1+	3+/1+	3+/4+	NA	3+/2+	0	0	2+/2+	0	3+/3+	NA
24	COST	Sp>R	A/A/P	Scant	Rop>D	96	18	2+/1+/1+	3+/1+	3+/4+	NA	3+/2+	0	0	2+/3+	0	3+/3+	NA
25	COST	Sp>R>St	P/A/P	Scant	Rop>F	70	22	2+/1+/1+	3+/2+	3+/4+	NA	3+/2+	0	0	3+/3+	0	3+/4+	NA
26	COST	Sp>R	P/A/P	Scant	Rop>F	104	4	1+/1+/1+	2+/1+	3+/4+	NA	3+/4+	0	0	2+/2+	0	3+/4+	NA
27	RFP	St>Sp	A/A/A	Scant	D>Rop	66	0	1+/1+/0	0	3+/2+	2+/4+	0	0	0	1+/2+	0	1+/1+	NA
28	RFP	Sp>St>R	A/A/A	Moderate	F>Rop	30	1	1+/1+/1+	2+/1+	3+/4+	NA	0	0	0	2+/1+	0	1+/1+	NA

A = absent; COST = conjunctival stromal tumor; D = dense; F = fibril; FC = floret-type giant cell; HPF = high power field; L = lymphocyte; M = macrophage; MNC = multinucleated cell; NA = not available (tissue not sufficient for analysis); P = present; PC = plasma cell; R = round; RFP = reactive fibromyxoid proliferation; Rop = ropey; Sp = spindle; St = stellate; VC = vacuolated cell.

[a]Cell morphology is described in the order of predominance.

[b]Collagen pattern is described in the order of predominance.

[c]Inflammatory cell infiltrate is scored as follows: 0 = no inflammatory cells, 1+ = rare cells (1–5 cells/HPF), 2+ = mild (6–30 cells/HPF). 3+ = moderate (31–100 cells/HPF).

[d]Immunohistochemical staining is expressed as intensity (0 = no staining, 1+ = mild staining, 2+ = moderate staining, 3+ = strong staining) and percentage of immunoreactive cells (0 = no staining, 1+ = 1%–25%, 2+ = 26%–50%, 3+ = 51%–75%, 4+ = 76%–100%).

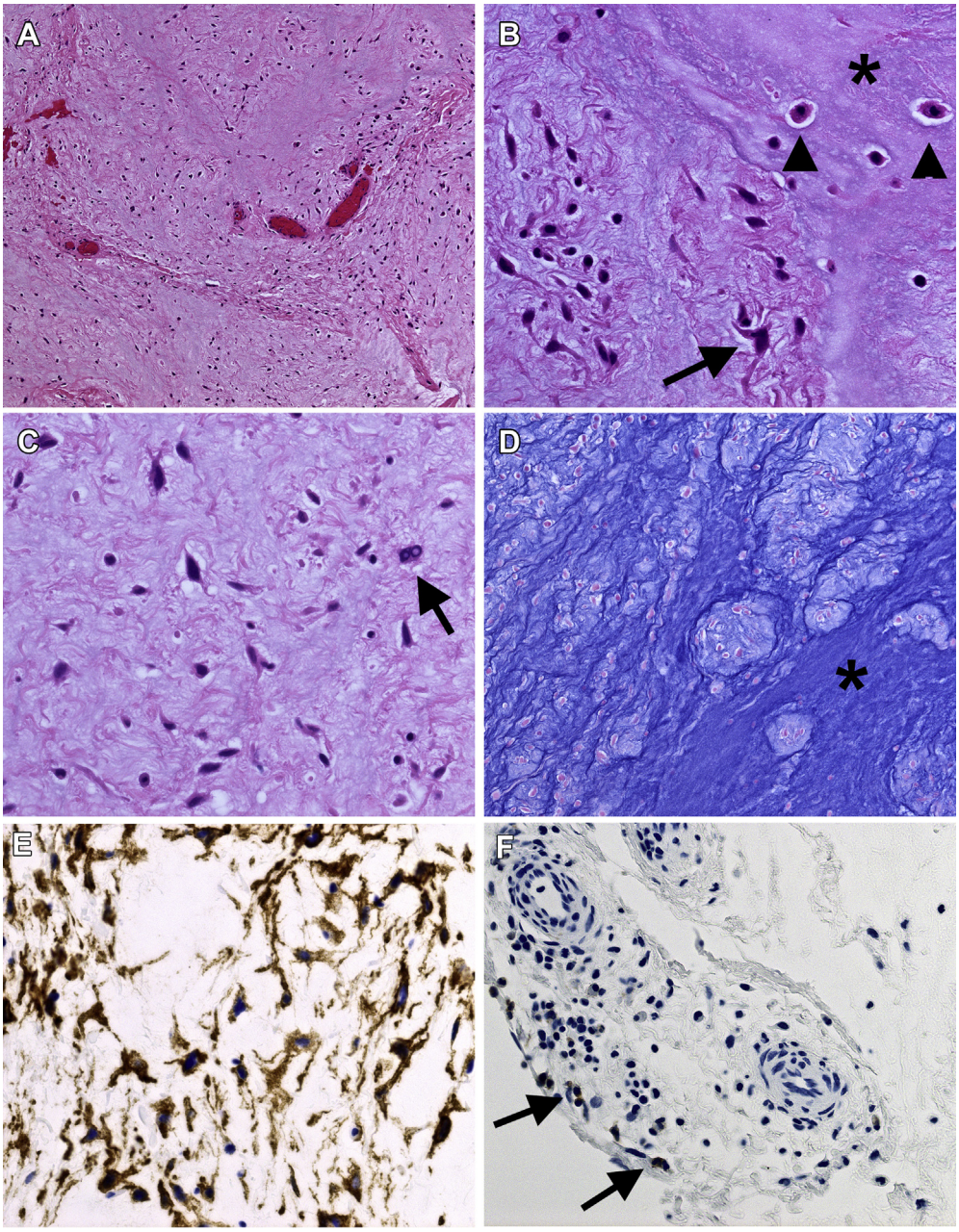

FIGURE 3. Pathologic features of Carney complex–associated conjunctival myxoma (Patient 1). A: At scanning magnification, the lesion is composed of scattered cells in an abundant myxoid matrix with scattered blood vessels (hematoxylin-eosin, x25 magnification). B: Higher magnification photomicrograph highlights that stellate cells (arrow) predominate in the lesion in a background of delicate fibrillary collagen, abundant myxoid matrix (asterisk), and scattered mast cells (arrowheads) (hematoxylin-eosin, x100 magnification). C: Occasional multinucleated cells with intranuclear pseudoinclusions (arrow) are noted (hematoxylin-eosin, x100 magnification). D: Alcian blue stain highlights abundant stromal mucin (asterisk) (Alcian blue, x50 magnification). E: CD34 immunostain labels the stromal cells in the lesion (CD34, x100 magnification). F: The lesional cells and blood vessels are negative for PRKAR1A with retained PRKAR1A expression in the lesional macrophages (arrows) (PRKAR1A, x100 magnification).

• **IMMUNOHISTOCHEMISTRY:** The immunohistochemical features of lesions are summarized in Table 2 and documented in Figures 3-7. All lesions evaluated by immunohistochemical stains demonstrated strong and diffuse immunoreactivity for CD34 and moderate-to-strong, diffuse immunoreactivity for vimentin. Scattered CD68-positive cells were noted in 19 of 22 lesions (86%). Factor XIIIa was expressed in scattered cells in 13

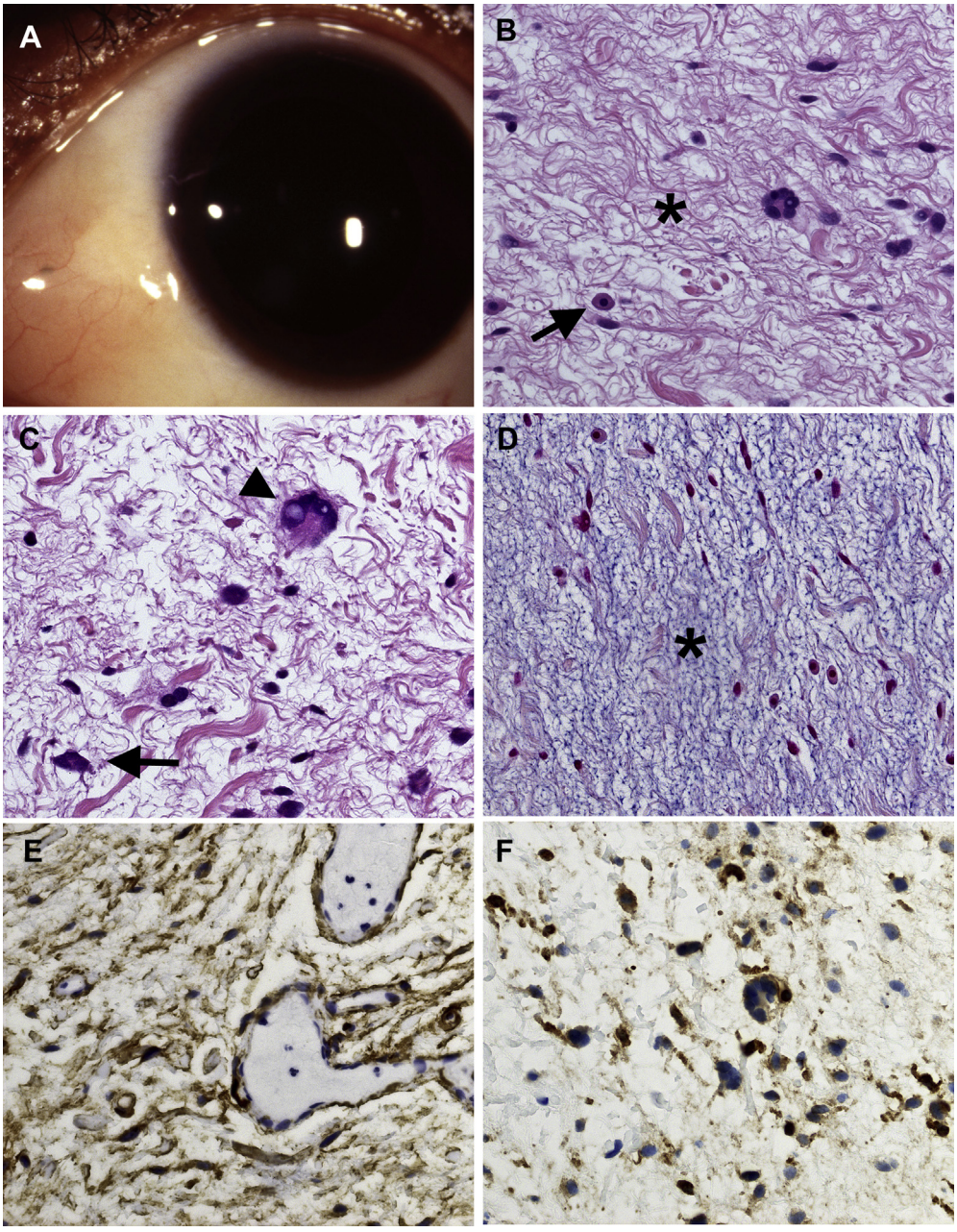

FIGURE 4. Clinical and pathologic features of morphologically typical, PRKAR1A-positive conjunctival myxoma (Patient 11). A: Gelatinous, translucent pink dome-shaped nodule in the nasal limbal and bulbar conjunctiva. B: Histopathology shows stellate, spindle, round, and multinucleated cells in a background of predominantly fibrillary collagen (asterisk), myxoid stroma, and scattered mast cells (arrow) (hematoxylin-eosin, x100 magnification). C: Higher magnification photomicrograph of the multinucleated cells with intranuclear pseudoinclusions (arrowhead) and stellate (multipolar) stromal cells (arrow) (hematoxylin-eosin, x200 magnification). D: Alcian blue stain highlights abundant stromal mucin (asterisk) (Alcian blue, x100 magnification). E: CD34 immunostain labels the stromal cells in the lesion and vascular endothelium (CD34, x100 magnification). F: The lesional cells express perinuclear and cytoplasmic PRKAR1A (PRKAR1A, x100 magnification).

of 21 lesions (62%). None of the lesions demonstrated immunoreactivity for S100 and SOX10 (performed to exclude myxoid peripheral nerve sheath tumors) and SMA (performed to exclude myofibroblastic and smooth muscle tumors). RB1 expression was retained in all evaluated lesions, arguing against the diagnosis of pleomorphic lipoma. The combined immunohistochemical pattern of expression in the lesions was compatible with a cellular proliferation derived from hematopoietic or dermal dendrocyte (CD34-, factor XIIIa-, and CD68-expressing)

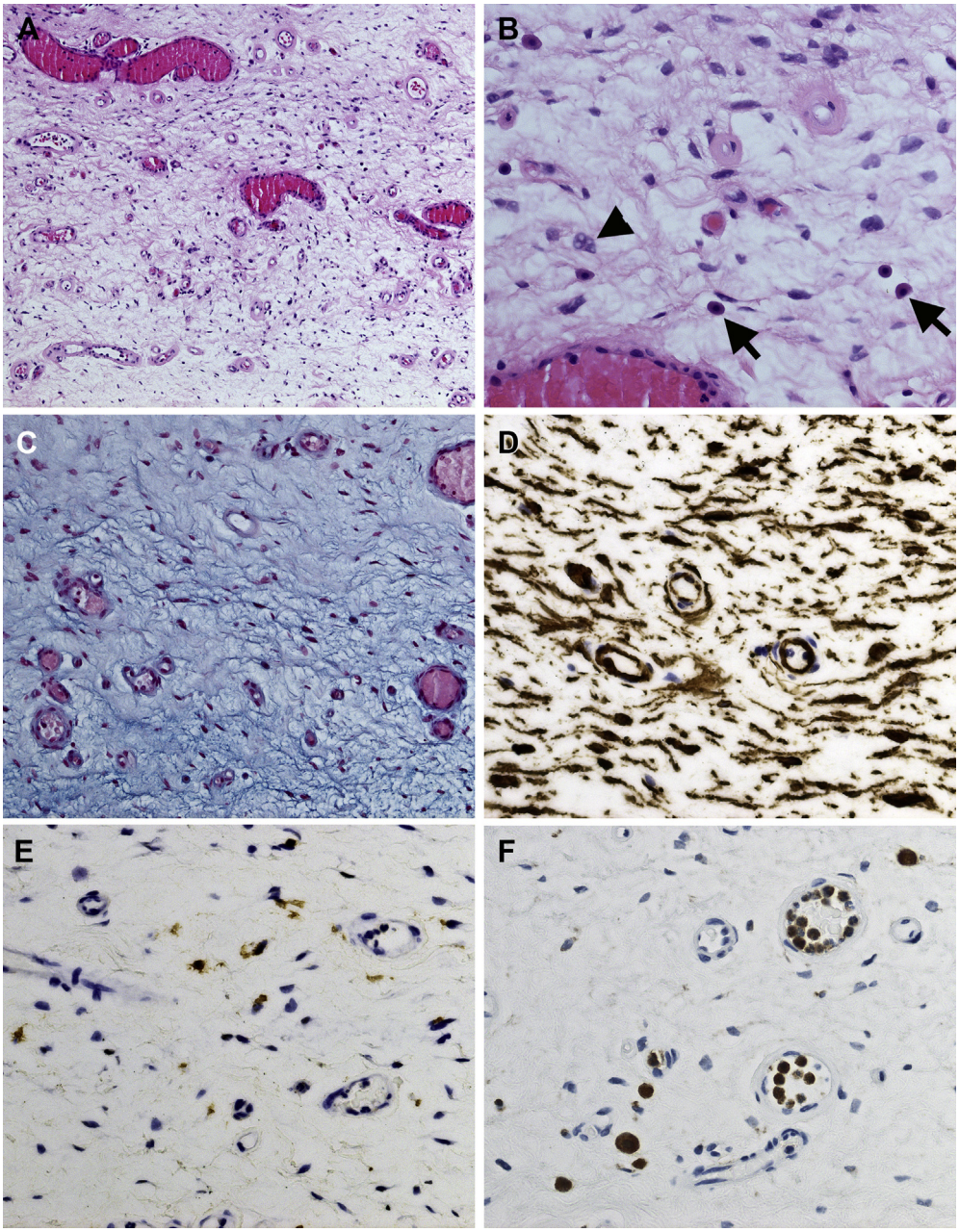

FIGURE 5. Pathologic features of morphologically typical, PRKAR1A-negative conjunctival myxoma (Patient 3). A: At scanning magnification, the lesion is composed of scattered cells in an abundant myxoid matrix, fibrillary collagen, and scattered blood vessels (hematoxylin-eosin, x25 magnification). B: Higher magnification photomicrograph highlights the stellate, round, and spindle cells, the occasional multinucleated cells with intranuclear cytoplasmic inclusions (arrowhead), and scattered mast cells (arrow) in a background of delicate fibrillary collagen and abundant myxoid matrix (hematoxylin-eosin, x100 magnification). C: Alcian blue highlights abundant myxoid matrix (Alcian blue, x50 magnification). D: CD34 immunostain labels the stromal cells in the lesion (CD34, x100 magnification). E: Factor XIIIa decorates the cytoplasm of occasional stromal cells (Factor XIIIa, x100 magnification). F: The lesional cells and blood vessels are negative for PRKAR1A, with retained PRKAR1A expression in the lesional inflammatory cells (PRKAR1A, x100 magnification).

and mesenchymal (vimentin-expressing) precursors. With intralesional inflammatory cells serving as internal positive controls, PRKAR1A expression was absent in 2 of 25 lesions (8%) (Figures 3 and 4), suggestive of genetic or epigenetic alterations in the *PRKAR1A* gene or posttranscriptional PRKAR1A protein modification.

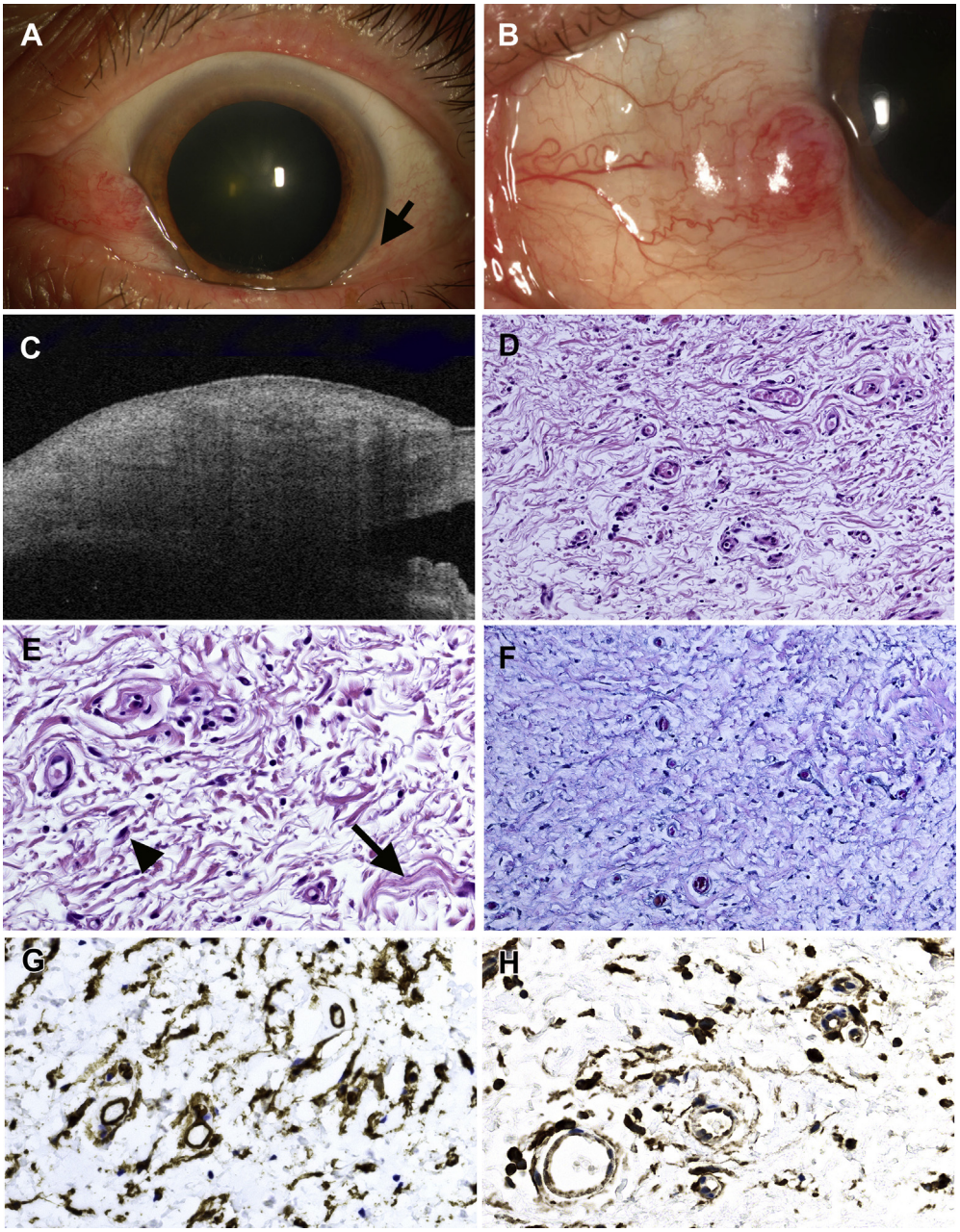

FIGURE 6. Clinical and pathologic features of a myxoid lesion with morphology compatible with conjunctival stromal tumor (Patient 12). A: Vascular nasal bulbar conjunctival mass associated with conjunctivochalasis (arrow). B: Variably vascular nasal limbal and bulbar mass with dense apex and gelatinous translucent base. C: Anterior segment optical coherence tomography demonstrates subepithelial conjunctival stromal mass with hyperreflectile anterior border and lucent center. D: At scanning magnification, the lesion is composed of scattered cells in moderate myxoid matrix, predominantly coarse ropey collagen, and scattered blood vessels (hematoxylin-eosin, x25 magnification). E: Higher magnification photomicrograph highlights the spindle cells with bipolar processes (arrowhead) that predominant the lesion and the occasional round cells, surrounded by predominantly coarse ropey collagen bundles (arrow) (hematoxylin-eosin, x100 magnification). F: Alcian blue highlights moderate myxoid matrix (Alcian blue, x50 magnification). G: CD34 immunostain labels the stromal cells in the lesion (CD34, x100 magnification). H: The lesional cells and blood vessels are positive for PRKAR1A (PRKAR1A, x100 magnification).

• ***PRKAR1A* GENE SEQUENCING:** The molecular genetic analysis results are summarized in Table 2. NGS performed on the 2 lesions with loss of PRKAR1A protein expression demonstrated a nonsense mutation involving the *PRKAR1A* gene (chromosome 17q24, CNC-1 locus, c.205C>T, p.Gln69*) with an allelic frequency of

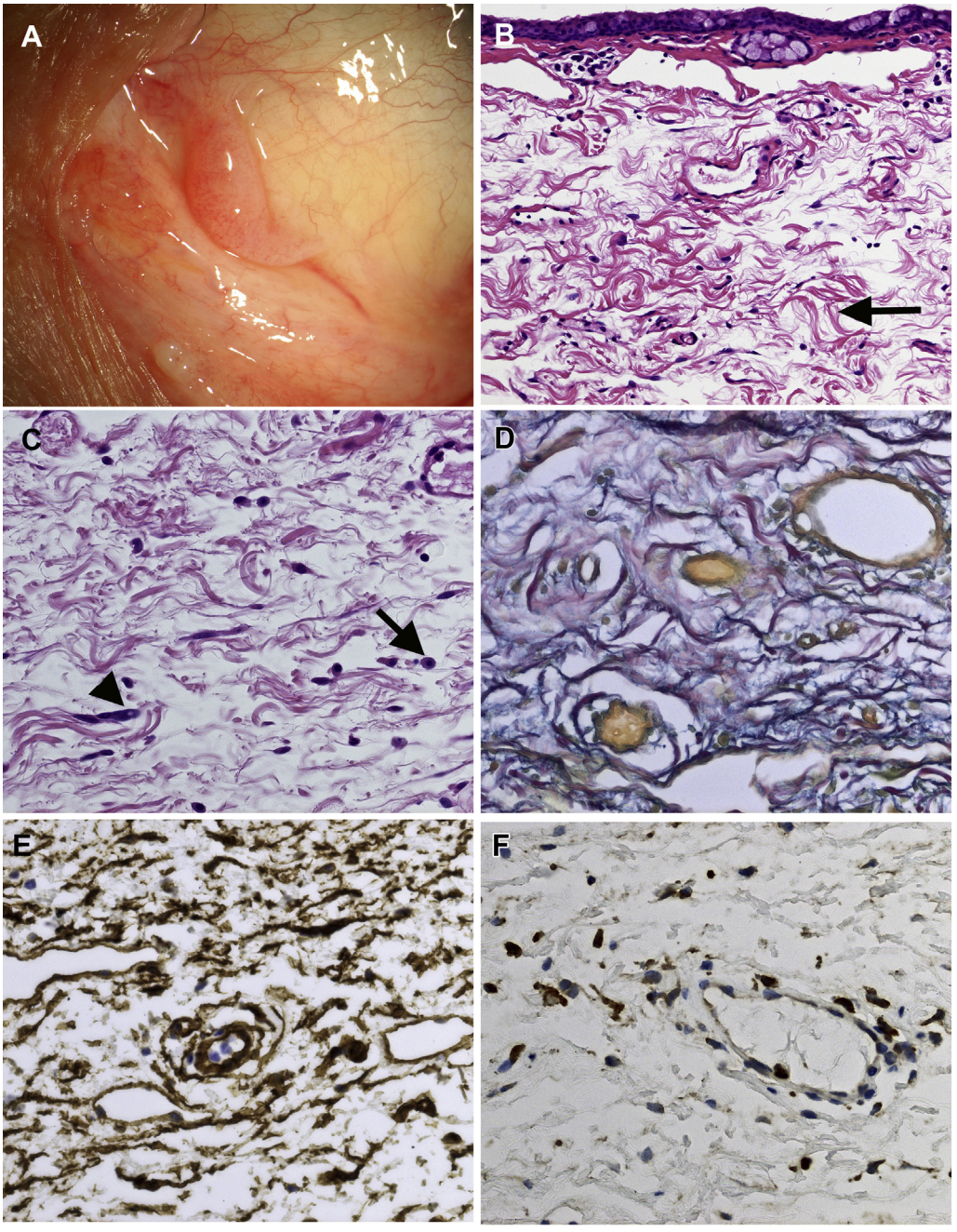

FIGURE 7. Clinical and pathologic features of myxoid lesion with morphology compatible with conjunctival stromal tumor (Patient 19). A: Finely vascular mass in plica semilunaris. B: At scanning magnification, the lesion is composed of scattered cells in a background of blood vessels and coarse ropey collagen bundles (arrow), separated by edema (hematoxylin-eosin, x25 magnification). C: Higher magnification photomicrograph highlights the spindle cells that predominate in the lesion with occasional intranuclear pseudoinclusions (arrowhead), surrounded by predominantly ropey collagen, and scattered mast cells (arrow) (hematoxylin-eosin, x100 magnification). D: Colloidal iron highlights scant myxoid matrix (Colloidal iron, x100 magnification). E: CD34 immunostain labels the stromal cells in the lesion (CD34, x100 magnification). F: The lesional cells and blood vessels are positive for PRKAR1A (PRKAR1A, x100 magnification).

~45% in the lesion from the patient with clinically documented CNC and no *PRKAR1A* sequence alterations in the second lesion from the patient with no clinical signs of CNC. However, absence of *PRKAR1A* sequence alterations could not be definitively excluded in the second lesion because of the low tumor percentage (20%). NGS

performed on the 2 lesions with retained PRKAR1A protein expression was negative for *PRKAR1A* sequence alterations.

• **ANALYSIS OF THE LESIONS BY PATHOLOGIC DIAGNOSIS:** Figures 2-6 depict the lesions originally diagnosed as myxoma. Figure 7 depicts the lesion originally diagnosed as COST. When analyzed by pathologic diagnosis, all tumors bearing the diagnosis of COST were localized to either the bulbar conjunctiva (not touching the corneoscleral limbus) or plica semilunaris and caruncle. In contrast, 12 of 15 (80%) tumors diagnosed as myxoma were juxtalimbal ($P = .02$). Of the 3 nonlimbal myxomas, 1 involved the tarsal conjunctiva and 2 involved the orbit—sites not involved in COST. Clinically, all myxomas appeared as cystic, translucent, or gelatinous dome-shaped nodules, and 3 of 8 COSTs (38%) had solid fibrovascular appearances ($P = .01$). On histopathologic analysis, stellate cells were more frequent in myxomas than COSTs (38% vs 0%, respectively; $P = .04$), and spindle cells were more frequent in COSTs than myxomas (100% vs 50%, respectively; $P = .02$). Ropey collagen was more common in COSTs than myxomas (60% vs 38%, respectively; $P = .04$), and fibrillary collagen predominated in myxomas (63%). The myxoid matrix was more abundant in myxomas than COSTs (70% vs 30%, respectively; $P = .01$). Inflammatory infiltrates were more intense in COSTs than myxomas (40% vs 7%, respectively; $P = .02$). On immunohistochemical analysis, immunoreactivity for factor XIIIa was noted in all lesions diagnosed as COST and 45% of tumors diagnosed as myxomas ($P = .002$). PRKAR1A expression was absent in 2 tumors diagnosed as myxoma, 1 of which carried a mutation in *PRKAR1A* and was a CNC-associated tumor.

There were no significant differences between tumors diagnosed as COSTs and myxomas with respect to patient age, sex, clinical history of cancer, ocular trauma and surface disease, symptoms duration, tumor size, other histopathologic parameters (vascular and mast cell density, nuclear cytoplasmic pseudoinclusions, multinucleated cells including floret-type giant cells), all other immunohistochemical parameters (including CD34, CD68, and vimentin), surgical management, and outcome.

Statistical analysis was not possible for the 2 lesions bearing the diagnosis reactive fibromyxoid proliferation. However, both lesions were characterized by cellular proliferations that lacked intranuclear cytoplasmic pseudoinclusions and multinucleated cells, which were present in >90% of presumed primary myxoid tumors. Mast cells were essentially absent in both lesions. A dense collagen arrangement was the dominant pattern in 1 reactive fibromyxoid proliferation, which was not evidenced in any other lesions in the study. In immunohistochemical stains, both lesions did not express factor XIIIa and had markedly decreased expression of PRKAR1A. Expression of other makers, including CD34, in immunohistochemical stains did not differ between reactive fibromyxoid proliferations and presumed primary myxoid tumors.

• **ANALYSIS OF LESIONS BY MORPHOLOGIC PARAMETERS:** Because of the inherent bias of the initial pathologic diagnosis and the immunohistochemical similarities in all evaluated tumors, we analyzed the lesions on the basis of morphology with respect to the amount of myxoid matrix, collagen, and cellular patterns.

Lesions with abundant myxoid matrix (14/28) occurred in younger patients of a mean age of 49 (median 50, range 23–68) years; lesions with scant-to-moderate myxoid matrix (14/28) occurred in patients of mean age 61 (median 63, range 18–82) years ($P = .04$). An additional exploratory analysis showed that lesions with abundant or moderate myxoid matrix were more likely to present clinically as gelatinous, translucent, or cystic dome-shaped nodules (Figures 1 and 5) than lesions with scant myxoid matrix (abundant or moderate 15/16 [94%] vs scant 3/6 [50%]; $P = .04$) (Figures 6 and 7). Involvement of the plica semilunaris or caruncle was seen only in the lesions with scant myxoid matrix (Figure 7), and involvement of the adjacent orbit was a feature found only in lesions with moderate-to-abundant myxoid matrix.

Lesions with abundant myxoid matrix were more likely than those with scant-to-moderate myxoid matrix to predominantly contain fibrillar collagen (13/14 [93%] vs 2/14 [14%], respectively; $P < .0001$) and stellate cells (6/14 [43%] vs 0/14 [0%], respectively; $P = .05$) (Figures 3-5). In contrast, lesions with scant-to-moderate myxoid matrix were more likely than those with abundant myxoid matrix to be predominantly composed of spindle cells (13/14 [93%] vs 7/14 [50%]; $P = .06$) in a background of ropey collagen (11/14 [79%] vs 1/14 [7%]; $P = .0001$) (Figures 6 and 7). Mild-to-moderate inflammatory infiltrates were more common in lesions with scant-to-moderate myxoid matrix (4/14, 29%) than those with abundant myxoid matrix (1/13, 8%), although the difference did not reach a statistical significance ($P = .33$).

Absence of PRKAR1A expression was seen only in lesions with abundant myxoid matrix and predominantly fibrillar collagen, containing stellate, spindle, and round cells (Figures 3 and 4). One of the 2 lesions demonstrated a mutation in the *PRKAR1A* gene in a patient with confirmed CNC (Figures 2 and 3).

No significant differences were seen between the lesions with abundant myxoid matrix composed predominantly of fibrillar collagen and lesions with scant-to-moderate myxoid matrix composed predominantly of ropey or dense collagen with respect to patient sex, clinical history of cancer, ocular trauma and surface disease, symptom duration, tumor size, other histopathologic parameters (vascular and mast cell density, nuclear cytoplasmic pseudoinclusions, multinucleation including floret-type giant cells), all other immunohistochemical parameters (including

CD34, factor XIIIa, CD68, and vimentin), surgical management, and risk for recurrence.

• **ANALYSIS OF LESIONS BY ASSOCIATION WITH CNC:** One of 28 lesions has been previously documented in a patient fulfilling the diagnostic criteria for CNC (Tables 1 and 2, Figures 2 and 3, Supplemental Table).[4] When compared with the other lesions in this study, the CNC-associated myxoma was diagnosed in a young patient (23 years vs mean 55 years and median 58 years), was the largest tumor in this series (20 mm vs mean 9 mm and median 8 mm), and was the only tumor associated with a concurrent myxoma of the eyelid skin. In addition, the CNC myxoma was the only tumor in this series localized to the tarsal conjunctiva and 1 of the 2 myxomas that had an orbital component.

Morphologically, the CNC myxoma was composed of stellate, spindle, and round cells suspended in abundant myxoid matrix with intervening predominantly fibrillar collagen, small caliber vascular channels with focal perivascular lymphoplasmacytic and macrophagic inflammatory infiltrates, and scattered mast cells (Figure 3).

In immunohistochemical stains, the CNC myxoma demonstrated immunoreactivity for CD34 and lacked expression of PRKAR1A, with intralesional inflammatory cells serving as an internal positive control (Figure 3). NGS confirmed the heterozygous pathogenic mutation in the *PRKAR1A* gene at the CNC-1 locus.

• **ANALYSIS OF THE LESIONS BY ASSOCIATION WITH TRAUMA, OCULAR SURFACE DISEASE, AND SYSTEMIC CONDITIONS:** Of the 14 patients who had a well-documented ocular history, 8 had a history of surgical or nonsurgical trauma to the conjunctiva or ocular surface disease. There were no significant differences in the clinical, histopathologic, or immunohistochemical parameters of the lesions in the patients with ocular surface injury when compared with the cohort with no history of ocular surface disease or injury.

Of the 20 patients with a well-documented medical history, 5 had a history of other neoplasms or immune-mediated disease. There were no significant differences in the clinical, histopathologic, or immunohistochemical parameters of the lesions in the patients with ocular surface injury when compared with the cohort with no history of ocular surface disease or injury.

DISCUSSION

MYXOMAS ARE A HETEROGENEOUS GROUP OF CONNECTIVE tissue tumors derived from primitive mesenchyme that resemble Wharton jelly in the core of the umbilical cord. Myxomas arise chiefly in the heart, skin, subcutaneous and aponeurotic tissues, bones, and genitourinary system and are infrequent in the eyelid and orbit.[23] Myxomas are extremely rare in the conjunctiva, accounting for <0.2% of all conjunctival lesions, with <60 cases reported in the literature to date.[1,2,11,24–26]

Although the neoplastic nature of myxomas has been previously questioned, its association with multiple endocrine neoplasia syndromes and recent molecular genetic data firmly establish the myxoma's identity as a true neoplasm. The syndromic associations and the accompanying molecular genetic alterations in myxomas are site dependent. Although mutations in the *GNAS1* gene have been identified in intramuscular myxomas associated with McCune-Albright and Mazabraud syndromes, cardiac, cutaneous (including eyelid), and mucosal (including conjunctival) myxomas are features of CNC associated with mutations in the *PRKAR1A* gene.[12,13,27,28]

A myxoma can be the presenting sign of CNC.[12] Additionally, the ophthalmic manifestations of CNC (eyelid myxoma and spotty pigmentation of the eyelids and caruncle) have been shown to precede the embolic events originating from cardiac myxoma.[4,5] Thus, the importance of early accurate diagnosis and the need for appropriate systemic and genetic evaluation have been emphasized repeatedly in the published reports on conjunctival myxoma.[1,3–5] However, a literature review on conjunctival myxoma reveals only 2 cases with syndromic associations. One patient (included in this study) fulfilled the criteria for CNC.[4] The second patient, a 36-year-old man with a large superior bulbar conjunctival lesion extending into the orbit, had Zollinger-Ellison syndrome and a presumptive tenuous association with CNC.[5]

The rarity of documented systemic associations in conjunctival myxoid tumors raises a question regarding their etiology. Unlike myxomas of the heart, bone, and muscle that have established molecular genetic alterations recognized in both syndromic and sporadic tumors, myxoid lesions of the conjunctiva may be analogous to their cutaneous and oral mucosal counterparts, which are subdivided into neoplastic myxoma and degenerative or reactive mucinosis.[13,14,16–21,29] Mucinosis may be idiopathic, occur after trauma, or be seen in a setting of systemic inflammatory disease and demonstrates morphologic and immunohistochemical similarities to myxomas.[16–21,29]

The hypothesis that a subset of conjunctival myxoid tumors may be reactive in nature has been raised by Herwig and associates, who described 4 lesions composed of spindle-shaped cells with pseudonuclear inclusions and occasional multinuclear cells in a background of myxoid-to-collagenous stroma. The tumors stained positive for CD34 and vimentin and focally for CD68 and factor XIIIa. The authors proposed that lesions with higher cellularity immunopositive for CD34 (not identified in some conjunctival myxomas) were a distinct entity, which they termed COST.[9] Herwig and associates noted that the bulbar conjunctival location of all lesions and reddish coloration in a setting of blepharitis in 2 lesions suggested an

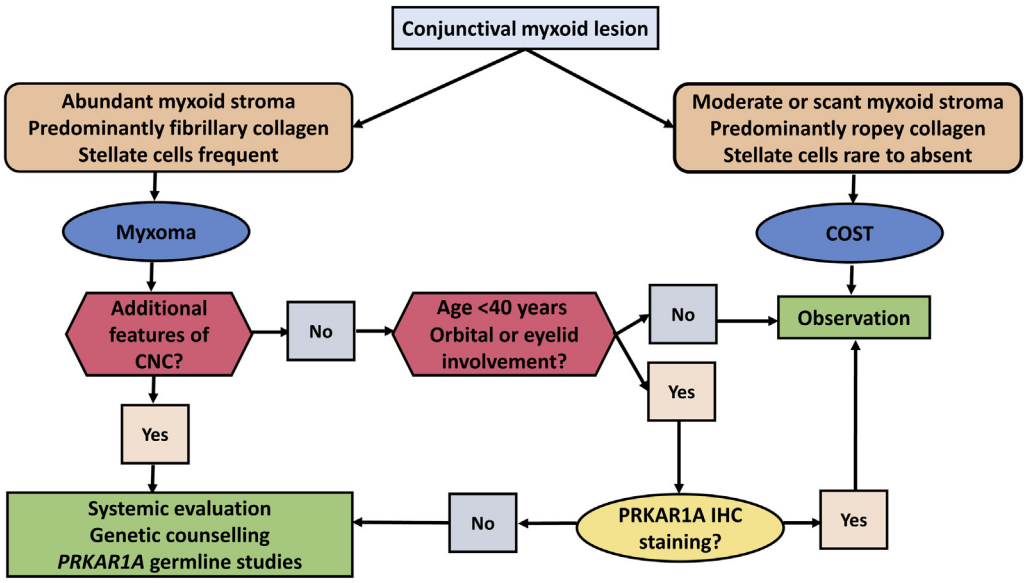

FIGURE 8. Potential diagnostic algorithm for conjunctival myxoid lesions. In the first step, morphologic evaluation enables differentiation between myxomas and COSTs in stratification of these lesions. Lesions not fulfilling the morphologic criteria for myxoma may be classified as COSTs. Patients with lesions fulfilling morphologic criteria for myxoma may be evaluated for additional features of CNC (Supplemental Table) via targeted personal and family medical history questionnaire. In patients with additional features of CNC, appropriate clinical evaluation, genetic counselling, and molecular genetic testing is recommended. In patients without additional features of CNC, PRKAR1A IHC stain may be a cost-effective method to screen for *PRKAR1A* mutations in tumors with an orbital or eyelid component and in lesions occurring before 4th decade (on the basis of the median age of CNC presentation being ~20 years and the age of 2 patients with documented syndromic conjunctival myxoma).[4,5,12] In tumors without PRKAR1A expression by IHC, *PRKAR1A* germline mutation studies may be undertaken. If the tumor is positive for PRKAR1A by IHC stain, it is unlikely to be occurring in the setting of CNC, and observation is recommended. CNC = carney complex; COST = conjunctival stromal tumor; IHC = immunohistochemical.

inflammatory or reactive pathogenesis.[9] The recent study by Qin and associates, however, demonstrated overlapping clinical and histopathologic features and an identical immunophenotype for conjunctival myxoma and COST, leading the authors to suggest that the term "conjunctival myxoid stromal tumor" may be more appropriately descriptive of this entity.[11] Our data corroborate the findings by Qin and associates, supporting the conclusion that conjunctival myxoid lesions cannot be separated on the basis of the previously described immunophenotypic features. However, the term conjunctival myxoid stromal tumor, while appealing in its inclusiveness, does not distinguish between the tumors with the potential for life-threatening syndromic associations and the myxoid lesions that are potentially reactive.

To distinguish between the neoplastic and reactive conjunctival myxoid tumors, one needs to synthesize the available clinical, morphologic, immunohistochemical, and molecular genetic data. According to Stout's classic morphologic definition of myxoma, this neoplasm is composed of stellate cells set in a loose myxoid stroma, through which course very delicate reticulin fibers in various directions, resembling primitive mesenchyme. Denser areas of thickened connective tissue with decreased myxoid material and spindle cells should not be extensive.[23] When we applied Stout's morphologic definition of myxoma to the conjunctival myxoid lesions in our series, we noted that such tumors occurred in younger patients and had a cystic or gelatinous appearance. Involvement of the tarsal conjunctiva, extension into the adjacent orbit, loss of PRKAR1A protein expression, and pathogenic mutation in the *PRKAR1A* gene were limited to the tumors that had a classic myxoma morphology.

Pathogenic mutations in the *PRKAR1A* gene, encoding the regulatory subunit type I alpha of cAMP-dependent protein kinase A (PKA), have been identified in >70% of patients with CNC, two-thirds of CNC cardiac myxomas, and one-third of isolated cardiac myxomas.[12,13] *PRKAR1A* haploinsufficiency leads to unrestrained catalytic subunit activity of PKA, resulting in increased cell proliferation in cAMP-responsive tissues and tumor formation.[12] Pathogenic *PRKAR1A* mutations typically are single base substitutions and small indels. However, large deletions and combined rearrangements also have been described. Additionally, activating pathogenic mutations and copy number gain in other subunits of PKA

(*PRKACA* and *PRKACB*) and linkage to another locus at 2p16 have been described in patients with CNC.

Maleszewski and colleagues reported that immunohistochemistry for PRKAR1A was useful in screening cardiac myxomas for CNC.[13] The investigators noted absence of PRKAR1A expression in all 7 CNC cases, and pathogenic *PRKAR1A* mutations in 67% of sequenced tumors. They observed that approximately one-third of isolated cardiac myxomas similarly were nonreactive for PRKAR1A, and 31% of nonsyndromic myxomas harbored pathogenic *PRKAR1A* mutations. The authors concluded that the lack of identifiable *PRKAR1A* mutations in cardiac myxomas that show negative immunoreactivity for PRKAR1A suggests that other mechanisms may play a role in their pathogenesis, including complex interactions from other areas of the genome, involvement at the gene level (either coding or regulatory modification), the epigenetic level (DNA hypermethylation), or the protein level (post-transcriptional modification).[13] Our study similarly confirms the role of *PRKAR1A* in pathogenesis of conjunctival myxoma. If one defines conjunctival myxoma by Stout's stringent morphologic criteria, 2 of 14 (14%) of conjunctival myxomas demonstrated loss of PRKAR1A protein expression, and the pathogenic *PRKAR1A* mutation was confirmed in 1 tumor associated with CNC.

One half of the lesions in our study lacked the classic morphology of myxoma. Morphologically similar to the COST described by Herwig and associates, these tumors were composed of spindle cells, with few to absent stellate cells, in a background of predominantly thick ropey collagen bundles and scant-to-moderate myxoid matrix.[9] These lesions were predominantly localized to the exposed interpalpebral region of the bulbar conjunctiva and plica semilunaris and caruncle, typically with a fibrovascular appearance clinically, raising the possibility of a reactive process, although no definitive association with ocular trauma, ocular surface disease, or systemic pro-inflammatory disease was identified in our patients. It is also notable that the 2 postsurgical reactive fibromyxoid proliferative lesions in our study appeared to be morphologically distinct from the other tumors, suggesting that different mechanisms are involved in the pathogenesis of these lesions. Although we cannot definitively exclude a neoplastic process in the tumors lacking the classic morphologic features of myxoma, it is possible that these lesions are analogous to solitary cutaneous focal mucinosis and oral focal mucinosis. Solitary focal mucinoses of the skin and oral mucosa share significant morphologic and immunohistochemical overlap with neoplastic myxoma, featuring scattered spindle fibroblasts in a background of mucin, mast cells, collagen fibers, and blood vessels.[16,29] The helpful morphologic features that distinguish solitary cutaneous focal mucinosis from myxoma include smaller lesion size, superficial location, and the presence of randomly arranged fragmented and ropey collagen fibers, which were similarly evident in the lesions in our study.[16]

Our data support the conclusion that at least a subset of conjunctival myxomas are true neoplasms and suggest that a subset of conjunctival myxoid lesions may be reactive. However, there is insufficient information to unequivocally distinguish between these pathologic processes on the basis of the parameters we considered in this study. The limiting factors include the small number of lesions in our study, reflecting the overall rarity of these tumors and the scarcity of tissue available for molecular genetic analysis.

Considering the published data and our study results, it may be prudent to reserve the term conjunctival myxoma to the lesions with classic morphology, as described by Stout. In such lesions, consideration of syndromic associations may be raised for large tumors with an orbital component, lesions associated with other ocular signs of CNC, and tumors occurring in younger patients (before the 4th decade, given the median age of ~20 years for CNC presentation and the age of 2 patients with documented syndromic conjunctival myxoma).[4,5,12] In selected cases, immunohistochemical staining for PRKAR1A may be a cost-effective method to screen for *PRKAR1A* mutations, followed by *PRKAR1A* germline mutation studies in patients with tumors demonstrating loss of PRKAR1A expression. The conjunctival lesions lacking classic morphologic features of myxoma may be either reactive or neoplastic in nature. The term COST with the term tumor applied in its original context of a mass lesion, as proposed by Herwig and associates, can be retained for these lesions. We anticipate that with continued refinement of our modern molecular genetic methods, we will be able to more definitively distinguish between the neoplastic and reactive myxoid conjunctival lesions. The potential diagnostic algorithm for conjunctival myxoid lesions is illustrated in the Figure 8.

Myxomas of nonophthalmic sites behave in a benign fashion, although local recurrences are not uncommon, particularly in CNC-associated tumors.[28] In our series, local recurrence was documented in a single incompletely excised myxoma associated with CNC and in 1 lesion fitting the morphologic criteria for COST. Therefore, complete excision of these lesions is recommended.

In summary, our study confirms that *PRKAR1A* plays a role in the development of a subset of syndromic and nonsyndromic conjunctival myxomas, particularly in tumors fulfilling the stringent morphologic criteria for myxoma. The term COST may be preferred for lesions not fulfilling the strict morphologic criteria for myxoma to avoid unnecessary systemic work-up. With the exception of PRKAR1A studies, the current immunohistochemical panels cannot reliably distinguish between conjunctival myxoma and COST. Thus, morphology remains the gold standard for diagnosis.

ALL AUTHORS HAVE COMPLETED AND SUBMITTED THE ICMJE FORM FOR DISCLOSURE OF POTENTIAL CONFLICTS OF INTEREST and none were reported. Funding/Support: This work was supported by the Filkins Family Foundation, Council Bluffs, IA and by the Eye Pathology Education and Research Fund, Wills Eye Hospital, Philadelphia, Pennsylvania. All authors attest that they meet the current ICMJE requirements to qualify as authors. This manuscript is based on a thesis that was prepared in partial fulfillment of the requirements for membership in the American Ophthalmological Society and published in the Transactions of the American Ophthalmological Society in 2019. The manuscript underwent subsequent peer review by the American Journal of Ophthalmology and has been modified following the peer review process.

REFERENCES

1. Xiong MJ, Dim DC. Conjunctival myxoma: a synopsis of a rare ocular tumor. *Arch Pathol Lab Med* 2015;139(5):693–697.
2. Ríos Y Valles-Valles D, Hernández-Ayuso I, Rodríguez-Martínez HA, et al. Primary conjunctival myxoma: case series and review of the literature. *Histopathology* 2017;71(4):635–640.
3. Demirci H, Shields CL, Eagle RC Jr, Shields JA. Report of a conjunctival myxoma case and review of the literature. *Arch Ophthalmol* 2006;124(5):735–738.
4. Kennedy RH, Flanagan JC, Eagle RC Jr, Carney JA. The Carney complex with ocular signs suggestive of cardiac myxoma. *Am J Ophthalmol* 1991;111(6):699–702.
5. Ramaesh K, Wharton SB, Dhillon B. Conjunctival myxoma, Zollinger-Ellison syndrome and abnormal thickening of the inter-atrial septum: a case report and review of the literature. *Eye (Lond)* 2001;15(3):309–312.
6. Pe'er J, Hidayat AA. Myxomas of the conjunctiva. *Am J Ophthalmol* 1986;102(1):80–86.
7. Pe'er J, Ilsar M, Hidayat A. Conjunctival myxoma: a case report. *Br J Ophthalmol* 1984;68(9):618–622.
8. Jain P, Finger PT, Iacob CE. Conjunctival myxoma: a case report with unique high frequency ultrasound (UBM) findings. *Indian J Ophthalmol* 2018;66(11):1629–1631.
9. Herwig MC, Wells JR, Grossniklaus HE. Conjunctival stromal tumor: report of 4 cases. *Ophthalmology* 2012;119(4):682–687.
10. Auw-Haedrich C, Danielewicz KD, Mendoza PR, Reinhard T, Grossniklaus HE. Conjunctival stromal tumor: expansion of findings in a newly described entity. *Ophthalmology* 2016;123(5):1166–1167.
11. Qin XY, Jin ZH, Wang YP, Zhang ZD. Conjunctival myxoid stromal tumour: a distinctive clinicopathological and immunohistochemical study. *Br J Ophthalmol* 2018;1–7.
12. Correa R, Salpea P, Stratakis CA. Carney complex: an update. *Eur J Endocrinol* 2015;173(4):M85–M97.
13. Maleszewski JJ, Larsen BT, Kip NS, et al. PRKAR1A in the development of cardiac myxoma: a study of 110 cases including isolated and syndromic tumors. *Am J Surg Pathol* 2014;38(8):1079–1087.
14. Perdigão PF, Stergiopoulos SG, De Marco L, et al. Molecular and immunohistochemical investigation of protein kinase a regulatory subunit type 1A (PRKAR1A) in odontogenic myxomas. *Genes Chromosomes Cancer* 2005;44(2):204–211.
15. Kacerovska D, Sima R, Michal M, et al. Carney complex: a clinicopathologic and molecular biological study of a sporadic case, including extracutaneous and cutaneous lesions and a novel mutation of the *PRKAR1A* gene. *J Am Acad Dermatol* 2009;61(1):80–87.
16. Kuo KL, Lee LY, Kuo TT. Solitary cutaneous focal mucinosis: a clinicopathological study of 11 cases of soft fibroma-like cutaneous mucinous lesions. *J Dermatol* 2017;44(3):335–338.
17. Verma G, Mrig PA, Gautam RK, Malhotra P. Trauma-induced focal nodular mucinoses: a rare entity. *Indian Dermatol Online J* 2018;9(1):50–52.
18. Martins C, Nascimento AP, Monte-Alto-Costa A, Alves Mde F, Carneiro SC, Porto LC. Quantification of mast cells and blood vessels in the skin of patients with cutaneous mucinosis. *Am J Dermatopathol* 2010;32(5):453–458.
19. Yokoyama E, Muto M. Adult variant of self-healing papular mucinosis in a patient with rheumatoid arthritis: predominant proliferation of dermal dendritic cells expressing CD34 or factor XIIIa in association with dermal deposition of mucin. *J Dermatol* 2006;33(1):30–35.
20. Sowmya GV, Manjunatha BS, Nahar P, Aggarwal H. Oral focal mucinosis: a rare case with literature review. *BMJ Case Rep* 2015;2015:1–3.
21. Gonzaga AK, de Oliveira DH, Lopes ML, Filho TJ, Queiroz LM, da Silveira ÉJ. Clinicopathological study of oral focal mucinosis: a retrospective case series. *Med Oral Patol Oral Cir Bucal* 2018;23(4):e401–e405.
22. Ida CM, Vrana JA, Rodriguez FJ, et al. Immunohistochemistry is highly sensitive and specific for detection of *BRAF* V600E mutation in pleomorphic xanthoastrocytoma. *Acta Neuropathol Commun* 2013;1:20.
23. Stout AP. Myxoma, the tumor of primitive mesenchyme. *Ann Surg* 1948;127(4):706–719.
24. Shields CL, Demirci H, Karatza E, Shields JA. Clinical survey of 1643 melanocytic and nonmelanocytic conjunctival tumors. *Ophthalmology* 2004;111(9):1747–1754.
25. Grossniklaus HE, Green WR, Luckenbach M, Chan CC. Conjunctival lesions in adults. A clinical and histopathologic review. *Cornea* 1987;6(2):78–116.
26. Shields CL, Alset AE, Boal NS, et al. Conjunctival tumors in 5002 cases. Comparative analysis of benign versus malignant counterparts. The 2016 James D. Allen lecture. *Am J Ophthalmol* 2017;173:106–133.
27. Walther I, Walther BM, Chen Y, Petersen I. Analysis of *GNAS1* mutations in myxoid soft tissue and bone tumors. *Pathol Res Pract* 2014;210(1):1–4.
28. Gošev I, Paić F, Durić Z, et al. Cardiac myxoma the great imitators: comprehensive histopathological and molecular approach. *Int J Cardiol* 2013;164(1):7–20.
29. Wilk M, Schmoeckel C. Cutaneous focal mucinosis–a histopathological and immunohistochemical analysis of 11 cases. *J Cutan Pathol* 1994;21(5):446–452.